Available online at www.sciencedirect.com

SCIENCE DIRECT

Regulatory Peptides 126 (2005) 55–59

REGULATORY PEPTIDES

www.elsevier.com/locate/regpep

Identification of ghrelin and its receptor in neurons of the rat arcuate nucleus

Muhtashan S. Mondal[a], Yukari Date[a], Hideki Yamaguchi[a], Koji Toshinai[a], Tomoko Tsuruta[a], Kenji Kangawa[b], Masamitsu Nakazato[a,*]

[a]*Third Department of Internal Medicine, Miyazaki Medical College, University of Miyazaki, Kiyotake, Miyazaki 889-1692, Japan*
[b]*Department of Biochemistry, National Cardiovascular Center Research Institute, Osaka 565-8565, Japan*

Available online 7 October 2004

Abstract

Ghrelin, an acylated peptide originally identified in rat stomach as the endogenous ligand for the growth hormone secretagogue receptor (GHS-R), stimulates both food intake and growth hormone (GH) secretion. Ghrelin is predominantly synthesized by a subset of endocrine cells in the oxyntic gland of human and rat stomach. Previous studies using immunohistochemistry have shown that ghrelin is also present in the hypothalamic arcuate nucleus, a region critical for the control of feeding and GH secretion, but its expression pattern in this region and the details of its molecular form has yet to be clarified. In this report, we examined the presence of ghrelin in the arcuate nucleus using reverse-phase liquid chromatography combined with radioimmunoassay (RIA) and immunohistochemistry. Neurons in the arcuate nucleus were observed to react positively to ghrelin antibodies. In addition, we confirmed the existence of ghrelin mRNA expression using the reverse-transcription polymerase chain reaction (RT–PCR). We also observed the colocalization of GHS-R with neuropeptide Y (NPY) and growth-hormone-releasing hormone (GHRH) in the arcuate nucleus. The present study clearly indicates that ghrelin is synthesized in the arcuate nucleus, which will further our understanding of ghrelin's actions in the central nervous system, including feeding behavior and GH secretion.

Keywords: Ghrelin; GHS-R; Arcuate nucleus; HPLC; RIA; Immunohistochemistry

1. Introduction

Ghrelin, a 28-amino acid peptide with an *n*-octanoyl modification that is indispensable for its activity, was originally discovered in human and rat stomach as an endogenous ligand for the growth hormone (GH) secretagogue receptor (GHS-R) [1]. Currently, ghrelin homologues have been identified in fish, amphibians, birds, and many mammals. Ghrelin is predominantly produced in the endocrine cells of the stomach and is then released into circulation. Gastrectomy in rats decreases plasma ghrelin concentrations by approximately 80%, indicating that the stomach is the main source of circulating ghrelin [2]. When administered either centrally or peripherally, ghrelin stimulates GH secretion, food intake, and body weight gain [1,3–8]. Several groups have demonstrated that intracerebroventricular administration of ghrelin induces food intake by way of neuropeptide Y (NPY) and agouti-related protein (AGRP) produced in the hypothalamic arcuate nucleus [8–10]. Central effects of ghrelin on feeding are also mediated in part by orexin-A and -B produced in the lateral hypothalamus [11]. These findings suggest that ghrelin is also synthesized in some regions of the brain involved in both feeding and GH secretion. We have already shown using immunohistochemistry that ghrelin-producing neurons are present in the arcuate nucleus, a region critical for feeding and GH secretion [1]. Further verification of the presence of ghrelin and its

Abbreviations: AGRP, agouti-related protein; CH_3CN, acetonitrile; GH, growth hormone; GHS-R, growth hormone secretagogue receptor; NPY, neuropeptide Y; RIA, radioimmunoassay; RP-HPLC, reverse-phase high-performance liquid chromatography; RT–PCR, reverse-transcription polymerase chain reaction.

* Corresponding author. Tel.: +81 985 85 7972; fax: +81 985 85 7902.
E-mail address: nakazato@med.miyazaki-u.ac.jp (M. Nakazato).

0167-0115/$ - see front matter © 2004 Elsevier B.V. All rights reserved.
doi:10.1016/j.regpep.2004.08.038

receptor in the arcuate nucleus would solidify current models of ghrelin's central activity.

In the present study, we analyzed and characterized ghrelin-immunoreactive molecules in the arcuate nucleus by reverse-phase high-performance liquid chromatography (RP-HPLC) combined with radioimmunoassay (RIA). Using immunohistochemistry, we investigated the ghrelin-immunoreactive neurons in the arcuate nucleus. We also examined the expression of ghrelin mRNA in the arcuate nucleus by reverse-transcription polymerase chain reaction (RT–PCR). We also studied the colocalization in neurons of the ghrelin receptor, GHS-R, with NPY and growth-hormone-releasing hormone (GHRH). Using these methods, we demonstrate that ghrelin is synthesized in the arcuate nucleus.

2. Materials and methods

2.1. Animals

Male Wistar rats weighing 300–350 g (Charles River Japan, Shiga, Japan) were used in all experiments. Rats, housed individually in plastic cages at constant room temperature in a 12-h light (07:00–19:00)/12-h dark cycle, were given standard laboratory chow and water ad libitum. All procedures were performed in accordance with the Japanese Physiological Society's guidelines for animal care. The protocol was approved by the Miyazaki Medical College Animal Care Research Committee.

2.2. Ghrelin radioimmunoassay (RIA)

Acylated ghrelin content was measured by radioimmunoassay (RIA) recognizing *n*-octanoylated ghrelin [12]. To generate anti-ghrelin antisera, synthetic [Cys^{12}]–ghrelin [1–11] peptide was conjugated to maleimide-activated mariculture keyhole limpet hemocyanin (mcKLH; Pierce, Rockford, IL). This antigenic conjugate solution was administered to three New Zealand white rabbits. The anti-rat ghrelin [1–11] antiserum (#G606) specifically recognized *n*-octanoylated ghrelin and did not recognize des-acyl ghrelin. Synthetic rat [Tyr^{29}]–ghrelin [1–28] was radioiodinated using the lactoperoxidase method. The ^{125}I-labeled peptide was purified on a TSK ODS SIL 120A column by RP-HPLC. Diluted samples or standard peptide solutions (100 μl) were incubated for 24 h with 100-μl diluted antiserum (final dilution of anti-ghrelin [1–11] antiserum, 1:620,000). Following addition of the tracer solution (16,000 cpm in 100 μl), mixtures were incubated for 24 h. Samples were assayed in duplicate; all procedures were done at 4 °C. The limit of detection of rat ghrelin [1–28] on the standard RIA curve was 0.5 fmol per tube. The respective intra- and interassay coefficients of variation at 50% binding for ghrelin RIA were 3.5% and 3.2%. The recoveries of rat ghrelin [1–28] (1 ng) and ^{125}I-rat ghrelin [1–28] (5000 cpm) added to the plasma samples extracted using Sep-Pak C-18 cartridges were 92.2±0.4% (S.E.M.) and 88.9±0.6% (S.E.M.), respectively.

2.3. Quantification of ghrelin in arcuate nucleus

Arcuate nuclei were punched out from the brains of 50 male Wistar rats following anesthesia with pentobarbital (Nembutal, Abbot Laboratories, Chicago, IL) after an overnight 12-h fast. These samples were then boiled at 100 °C for 3 min and applied to a Sep-Pak cartridge. The eluates were subjected to ghrelin RIA, as described above. Portions of the Sep-Pak eluates were applied to RP-HPLC on a TSK ODS SIL 120A column (4.6×150 mm, Tosoh, Tokyo, Japan). RP-HPLC was performed for 40 min at 1.0 ml/min with a linear gradient of acetonitrile (CH_3CN; 10–60%) in 0.1% TFA. All HPLC fractions were quantified by ghrelin RIA.

2.4. Preparation of anti-GHS-R serum

A [Cys0]-rat GHS-R [342–364] peptide was synthesized using the Fmoc solid-phase method on a peptide synthesizer (433A, Applied Biosystems, Foster City, CA) and then purified by RP-HPLC. The synthesized peptide (10 mg) was conjugated to maleimide-activated mariculture keyhole limpet hemocyanin (mcKLH, Pierce; 6 mg) in conjugation buffer (Pierce). The conjugate was emulsified with an equal volume of Freund's complete adjuvant and used to immunize New Zealand white rabbits by intra- and subcutaneous injection. Animals were boosted every 2 weeks and bled 7 days after each injection. The specificity of the antiserum was confirmed by its immunoreactivity against GHS-R-expressing (CHO-GHSR62 cells) but not control cells.

2.5. Immunohistochemistry

Three male Wistar rats weighing 250–300 g were used for immunohistochemical study. To enhance the immunostaining of GHS-R-expressing neurons, colchicine (100 μg/rat) was injected into the lateral ventricle 30 h before perfusion. Rats were perfused transcardially with 0.1 M phosphate buffer (pH 7.4) and then with 4% paraformaldehyde in 0.1 M phosphate buffer. The hypothalamus was sectioned into 40-μm thick slices at −20 °C using a cryostat and then treated with 0.3% hydrogen peroxide for 1 h to inactivate endogenous peroxidases. The hypothalamic sections were incubated for 2 days at 4 °C, with anti-ghrelin antiserum diluted 1:1000 or with anti-GHS-R antiserum diluted 1:1000. The pituitary sections were incubated for 2 days at 4 °C with anti-GHS-R antiserum diluted 1:1000. All of the sections were stained using the avidin–biotin complex method, as described previously [13]. We subsequently performed double staining for GHS-

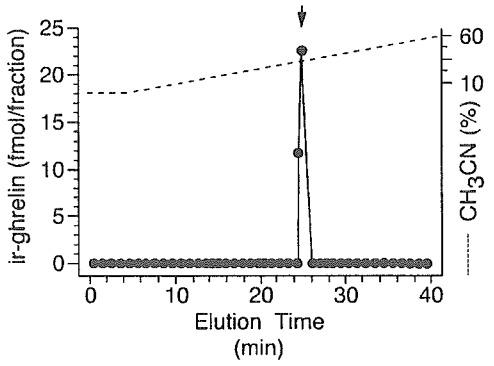

Fig. 1. Representative RP-HPLC profile of ghrelin extracted from rat arcuate nucleus. Wet weight (250 mg) of rat arcuate nucleus was analyzed. Arrow indicates the elution position of *n*-octanoylated ghrelin.

R vs. either NPY or GHRH in some sections of the hypothalamic arcuate nucleus. We also performed double staining for GHS-R vs. GH in some sections of the anterior pituitary. After the sections of arcuate nucleus and anterior pituitary were stained with anti-NPY antiserum (Diasorin, Stillwater, MN; final dilution 1:500) or anti-GHRH antiserum (Chemicon International, Temecula, CA; final dilution 1:1000) and with anti-GH antiserum (NIDDK, National Hormone and Peptide Program, Torrance, CA; final dilution 1:5000), respectively, they were washed with 100 mM glycine–HCl buffer (pH 2.2). Next, the sections of arcuate nucleus and anterior pituitary were stained with anti-GHS-R antiserum using an SG (blue/gray) substrate kit (Vector Laboratories, Burlingame, CA). To test for antiseral specificity, preabsorption tests were done using anti-ghrelin that had been absorbed with 10 μg of ghrelin and GHS-R antiserum that had been absorbed with 10 μg of GHS-R.

2.6. RT–PCR for ghrelin

Total RNA was extracted from the arcuate nuclei of three Wistar rats by the acid guanidinium thiocyanate–phenol–chloroform (AGPC) method [14]. First-strand cDNA was synthesized from 2.5 μg RNA and 7 μM oligo-$(dT)_{18}$ primer with ReverTra Ace-α-™ (Toyobo, Osaka, Japan). The resulting cDNA was subjected to PCR amplification with 2 μM each of the sense and antisense primers and 2.5 units of Pyrobest DNA polymerase (Takara Shuzo, Shiga, Japan). PCR primers for ghrelin were 5′-TTGAGCCCAGAGCACCAGAAA-3′ (sense) and 5′-AGTTGCAGAGGAGGCAGAAGCT-3′ (antisense), corresponding to nucleotide numbers 112–132 and 437–458 (Reference 4, GenBank). PCR was conducted in a reaction volume of 25 μl for 35 cycles comprising denaturation for 5 s at 94°C, annealing for 10 s at 65 °C, and extension for 1 min at 72 °C. The PCR products were electrophoresed on a 2% agarose gel (FMC BioProducts, Rockland, ME).

3. Results

3.1. HPLC characterization of ghrelin-immunoreactive molecules and its content in the arcuate nucleus

RP-HPLC coupled with ghrelin RIA was used to analyze the presence of immunoreactive ghrelin molecules in the arcuate nucleus. A large peak corresponding to immunoreactive ghrelin was eluted at the position of *n*-octanoylated ghrelin in arcuate nucleus tissue extract (Fig. 1). The ghrelin content measured by RIA in the arcuate nucleus was 0.56 pg/mg tissue extract.

3.2. Immunohistochemistry

Neuronal cell bodies immunoreactive for ghrelin were found in the arcuate nucleus (Fig. 2A and B). No immunoreactivity for ghrelin was detected in the arcuate nucleus when normal rabbit serum or antisera preabsorbed with an excess of ghrelin was applied (data not shown). Neurons immunostained with GHS-R antisera were also present in the arcuate nucleus (Fig. 3A). GHS-R immunoreactivity colocalized with that of NPY (Fig. 3B) and GHRH (Fig. 3C) in some neurons in the arcuate nucleus. GHS-R was also abundantly expressed in the pituitary,

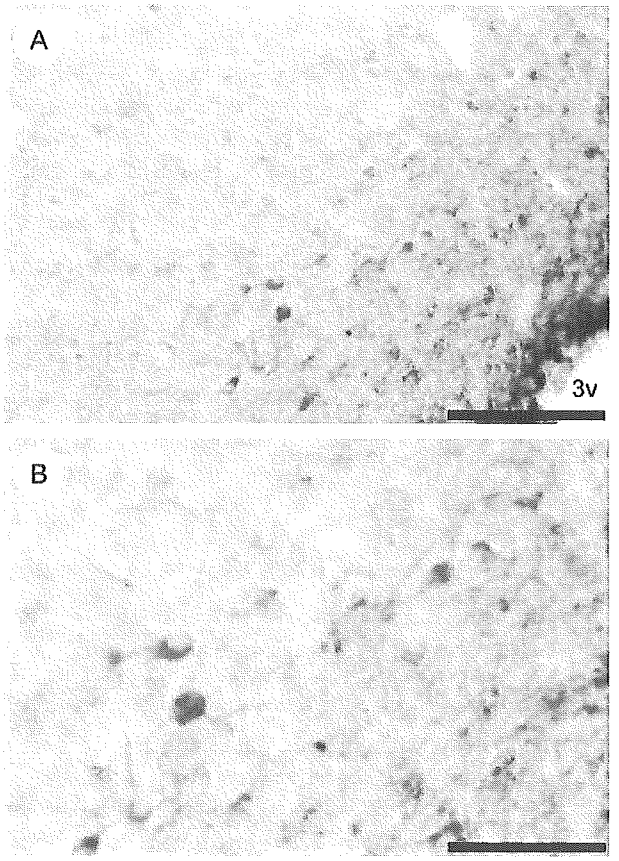

Fig. 2. Immunohistochemical localization of ghrelin in the arcuate nucleus. (A) Ghrelin-immunoreactive neurons in the arcuate nucleus. Bar, 50 μm. (B) High magnification of panel (A). Bar, 25 μm.

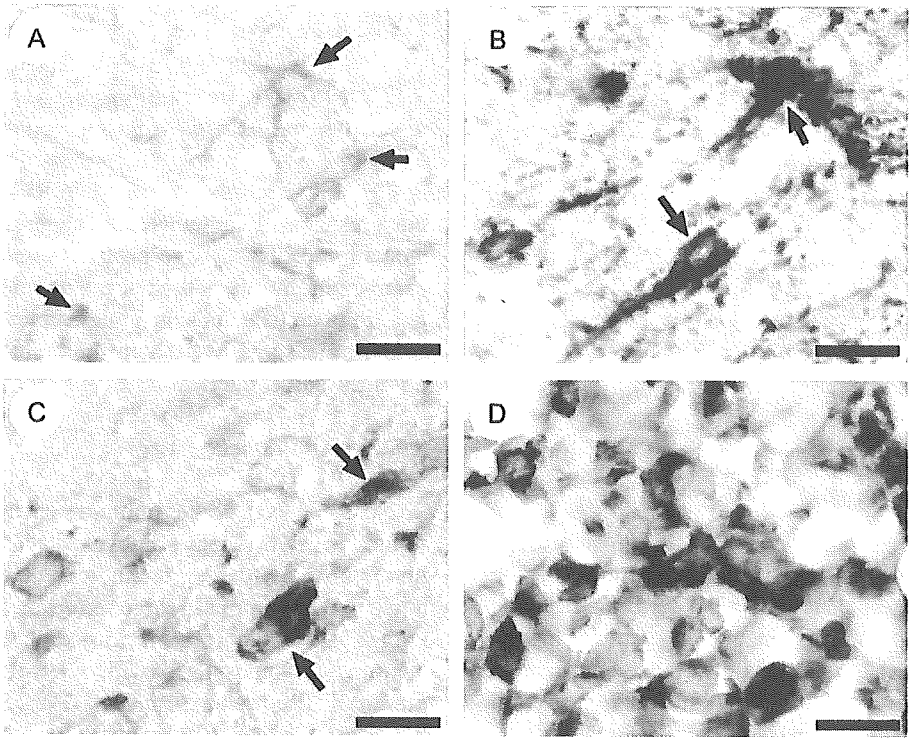

Fig. 3. Immunohistochemical localization of GHS-R in arcuate nucleus and the anterior pituitary. (A) GHS-R-immunoreactive neurons in the arcuate nucleus (arrows). (B) GHS-R-immunoreactive neurons (blue-black) colocalized with NPY neurons (brown; arrows) and (C) GHRH neurons (brown; arrows) in the arcuate nucleus. (D) GHS-R-immunoreactive cells (blue-black) colocalized with GH-producing cells (brown) in the pituitary. Bar, 20 μm in panel (A) to panel (D). (For interpretation of the references to colour in this figure legend, the reader is referred to the web version of this article.)

where it colocalized with GH-producing cells (Fig. 3D). No GHS-R immunoreactivity was detected in the arcuate nucleus or pituitary gland when normal rabbit serum or antisera preabsorbed with an excess of GHS-R was applied (data not shown).

3.3. RT–PCR amplification of ghrelin transcript

Using ghrelin-specific primers, an RT–PCR product corresponding to the predicted 347-bp size of the ghrelin transcript was present in a rat arcuate nucleus RNA sample (Fig. 4, left panel) but not present when no template was used in the reaction (Fig. 4, right panel).

4. Discussion

Ghrelin is a recently discovered gastrointestinal hormone that appears to play a major role in regulating energy balance [1,3–8]. Ghrelin is predominantly produced in the X/A-like cells of the stomach and may link the gastrointestinal system with hypothalamic control of energy balance, growth, and digestive functions [15]. Central administration of ghrelin has been shown to stimulate GH secretion as well as food intake, fat deposition, and body growth [1,3–8]. Central administration of ghrelin also activates various nuclei in rat hypothalamus, including critical regions for GH and energy homeostasis [8]. These findings strongly suggest the existence of neurons that produce ghrelin and/or its receptor in the brain. In situ hybridization histochemistry has demonstrated expression of the mRNA encoding the ghrelin receptor GHS-R in the pituitary, hypothalamus, pancreas, stomach, and other tissues [16], but immunohistochemical localization of GHS-R has yet to be confirmed.

The present study shows that ghrelin-immunoreactive neurons exist in the ventral portion of the arcuate nucleus, which is consistent with a previous published report [1]. Furthermore, we demonstrated ghrelin immunoreactivity in the arcuate nucleus using RP-HPLC combined with RIA. Ghrelin mRNA expression was also found in the arcuate nucleus. These results imply that the arcuate nucleus may be a major source of ghrelin in the central nervous system of rats. In addition, GHS-R was expressed in NPY- and

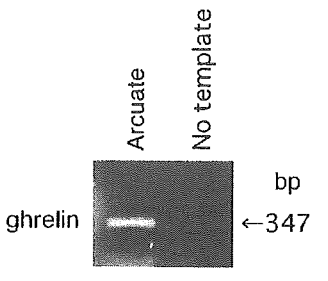

Fig. 4. Representative agarose gel showing the RT–PCR product corresponding to ghrelin mRNA amplified from rat arcuate nucleus.

GHRH-immunoreactive neurons of the rat arcuate nucleus, suggesting that central ghrelin directly affects these neurons which enhance feeding and GH secretion. We also demonstrated that GH-producing cells in the anterior pituitary express GHS-R. This finding indicates that ghrelin also induces GH secretion via an endocrine as well as a neural pathway.

In summary, the present study demonstrated the expression of an active *n*-octanoylated form of ghrelin in the arcuate nucleus. Given the expression of GHS-R in NPY- and GHRH-producing neurons, central ghrelin is expected to play an important role in appetite stimulation, energy homeostasis, and GH secretion. Such identification of ghrelin in the brain will facilitate the investigation of the link between peripheral factors relaying starvation or satiety signals and central ghrelin pathways. Further examination of the distribution of GHS-R-immunoreactive cells throughout the brain and peripheral tissues could lead to discovery of novel functions of ghrelin.

Acknowledgments

This study was supported in part by The 21st Century COE Program and grants-in-aid from the Ministry of Education, Culture, Sports, Science, and Technology, Japan to M.N.

References

[1] Kojima M, Hosoda H, Date Y, Nakazato M, Matsuo H, Kangawa K. Ghrelin is a novel growth hormone releasing acylated peptide from stomach. Nature 1999;402:656–60.

[2] Dornville de la Cour C, Bjorkqvist M, Sandvik AK, Bakke I, Zhao CM, Chen D, et al. A-like cells in the rat stomach contain ghrelin and do not operate under gastrin control. Regul Pept 2001;99:141–50.

[3] Tschöp M, Smiley DL, Heiman M. Ghrelin induces adiposity in rodents. Nature 2000;407:908–13.

[4] Wren AM, Small CJ, Ward HL, Murphy KG, Dakin CL, Taheri S, et al. The novel hypothalamic peptide ghrelin stimulates food intake and growth hormone secretion. Endocrinology 2000;141:4325–8.

[5] Takaya K, Ariyasu H, Kanamoto N, Iwakura H, Yoshimoto A, Harada M, et al. Ghrelin strongly stimulates growth hormone release in humans. J Clin Endocrinol Metab 2000;85:4908–11.

[6] Seoane LM, Tovar S, Baldelli R, Arvat E, Ghigo E, Casanueva FF, et al. Ghrelin elicits a marked stimulatory effect on GH secretion in free-moving rats. Eur J Endocrinol 2000;143:R007–9.

[7] Asakawa A, Inui A, Kaga T, Yuzuriha H, Nagata T, Ueno N, et al. Ghrelin is an appetite-stimulatory signal from stomach with structural resemblance to motilin. Gastroenterology 2001;120:337–45.

[8] Nakazato M, Murakami N, Date Y, Kojima M, Matsuo H, Kangawa K, et al. A role for ghrelin in the central regulation of feeding. Nature 2001;409:194–8.

[9] Shintani M, Ogawa Y, Ebihara K, Aizawa-Abe M, Miyanaga F, Takaya K, et al. Ghrelin, an endogenous growth hormone secretagogue, is a novel orexigenic peptide that antagonizes leptin action through the activation of hypothalamic neuropeptide Y/Y1 receptor pathway. Diabetes 2001;50:227–32.

[10] Kamegai J, Tamura H, Shimizu T, Ishii S, Sugihara H, Wakabayashi I. Chronic central infusion of ghrelin increases hypothalamic neuropeptide Y and Agouti-related protein mRNA levels and body weight in rats. Diabetes 2001;50:2438–43.

[11] Toshinai K, Date Y, Murakami N, Shimada M, Mondal MS, Shimbara T, et al. Ghrelin-induced food intake is mediated via the orexin pathway. Endocrinology 2003;144:1506–12.

[12] Hosoda H, Kojima M, Matsuo H, Kangawa K. Ghrelin and des-acyl ghrelin: two major forms of rat ghrelin peptide in gastrointestinal tissue. Biochem Biophys Res Commun 2000;279:909–13.

[13] Date Y, Ueta Y, Yamashita H, Yamaguchi H, Matsukura S, Kangawa K, et al. Orexins, orexigenic hypothalamic peptides, interact with autonomic, neuroendocrine and neuroregulatory systems. Proc Natl Acad Sci U S A 1999;96:748–53.

[14] Chomczynski P, Sacchi N. Single-step method of RNA isolation by acid guanidinium thiocyanate–phenol–chloroform extraction. Anal Biochem 1987;162:156–9.

[15] Date Y, Kojima M, Hosoda H, Sawaguchi A, Mondal MS, Suganuma T, et al. Ghrelin, a novel growth hormone-releasing acylated peptide, is synthesized in a distinct endocrine cell type in the gastrointestinal tracts of rats and humans. Endocrinology 2000;141:4255–61.

[16] Guan X-M, Yu H, Palyha OC, McKee KK, Feighner SD, Sirinathsinghji DJ, et al. Distribution of mRNA encoding the growth hormone secretagogue receptor in brain and peripheral tissues. Brain Res Mol Brain Res 1997;48:23–9.

Peptide Science 2004 : Y. Shimohigashi (Ed.)
The Japanese Peptide Society (2005)

Peptidome Database and Identification of New Endogenous/Bioactive Peptides

Naoto Minamino[1], Hiromiki Kuwahara[1], Yasuko Kuwahara-Matsui[1], Junko Isoyama-Tanaka[1], Takahiro Kihara[1], Masami Matsubae[1,2], Takeshi Katafuchi[1], Toshifumi Takao[2], and Masaharu Isoyama[3]

[1]National Cardiovascular Center Research Institute, Suita, Osaka 565-8565, Japan
[2]Institute for Protein Research, Osaka University, Suita, Osaka 565-0871, Japan, and
[3]Protein Research Foundation, Toyonaka, Osaka 560-0082, Japan
e-mail: minamino@ri.ncvc.go.jp

Peptidome database is aimed to comprehensively accumulate the fact data for the peptides present in the specific cells, tissues and organisms. In this database, the peptide data are stored based on their hydrophobicity, charges and molecular masses. By minimizing the degradation, the data are deduced to reflect the endogenous forms of the peptides. Thus, this database is expected to provide a new basement for peptide research, especially for identifying new endogenous and bioactive peptides.

Keywords: peptidome, fact database, endogenous peptides, 2-dimensional HPLC, mass spectrometry.

Introduction

Peptides play crucial roles in many physiological events as hormones, neurotransmitter and local mediators, but no database for endogenous peptides is available. This is mainly due to the following facts; i) peptide contents are extremely low, ii) most peptides in the cells are degradation products of proteins, and iii) peptides are easily susceptible to proteolysis during extraction and purification. Moreover, peptides are generated from precursor proteins by specific cleavages, and the cleavage sites are often different in different tissues. Modification of the peptides, such as amidation, is also essential for eliciting biological activity. As the processing, including cleavage and modification, is the most important feature of bioactive peptides and is difficult to deduce from the DNA sequences, fact data for endogenous peptides must be accumulated in order to advance peptide research.

Despite these problems and difficulties, we demonstrated that endogenous peptides can be detected at substantial levels by minimizing the degradation of proteins and peptides. By separating peptides by 2-dimensional (2D) chromatography composed of ion exchange and reverse phase high performance liquid chromatography (HPLC), a huge number of peptides were detected by the recently advanced mass spectrometers. In 1999, we undertook the Peptidome project, which is aimed to comprehensively analyze all peptides in the cells and tissues, to store the data based on

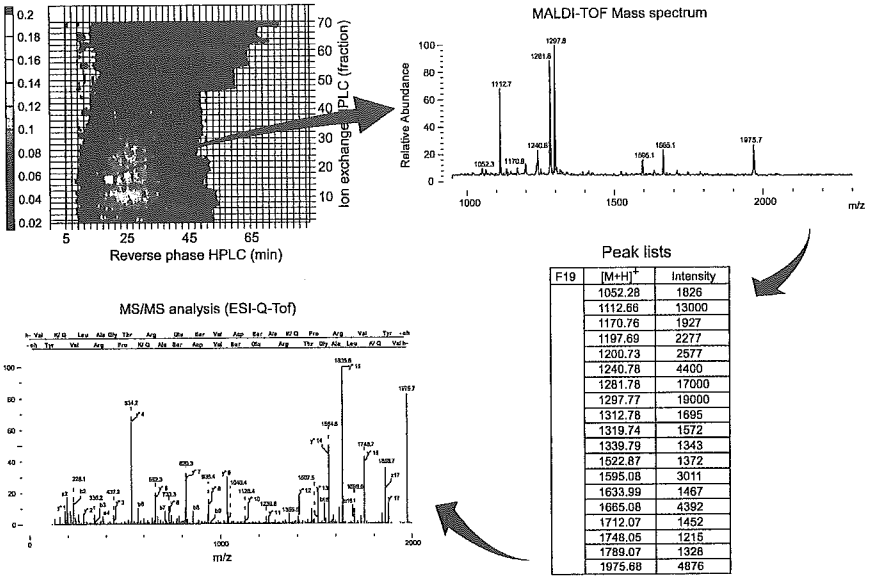

F19	$[M+H]^+$	Intensity
	1052.28	1826
	1112.66	13000
	1170.76	1927
	1197.69	2277
	1200.73	2577
	1240.78	4400
	1281.78	17000
	1297.77	19000
	1312.78	1695
	1319.74	1572
	1339.79	1348
	1522.87	1372
	1595.08	3011
	1633.99	1467
	1665.08	4392
	1712.07	1452
	1748.05	1215
	1789.07	1328
	1975.68	4876

Figure 1. Profiling procedures of the Peptidome database. Peptides are separated by the 2D-HPLC, and each fraction is submitted to the MS analysis. Major peaks are further analyzed by the tandem mass spectrometers.

the physiocochemical properties of peptides along with other related information [1].

Results and Discussion

Pig and mouse brain were collected immediately after sacrifice, diced and boiled in water for more than 5 min to inactivate proteases. After cooling, peptides were homogenized and extracted with 1 M acetic acid. The crude peptide fraction was prepared by the batch-wise treatment with C-18 resin and SP-Sephadex columns, which was separated by Sephadex G-50 gel filtration to remove remaining proteins. The peptide fraction was devided into two fractions of Mr<3,000 and 3,000<Mr<6,000. Each fraction was separated into 70 fractions by SP-2SW ion exchange HPLC with a linear gradient elution of $HCOONH_4$ (pH 3.8) from 10 mM to 1.0 M in the presence of 10% CH_3CN. Seventy fractions thus obtained were each subjected to reverse phase HPLC on a C-18 column with a linear gradient elution of CH_3CN in the presence of 0.1% trifluoroacetic acid (or formic acid), and separated into 75 fractions. By this 2D-HPLC system, peptides were separated into about 5,000 fractions, and an aliquot of each fraction was submitted to MALDI-TOF mass spectrometric (MS) analysis and peak lists of the peptides were stored. For *de novo* sequencing of the peptides, another aliquot was submitted to ESI-Q-TOF or MALDI-TOF-TOF MS analysis, and these data were stored in the database (Fig. 1).

In the course of the separation and analysis, degrees of hydrophobicity, net positive charges and molecular masses of the peptides are determined and estimated, which are employed as major parameters to register the peptide information in the Peptidome database, in addition to their sequences and names [1]. To normalize the 2D-HPLC system, we use a series of synthetic peptides of 11 amino acids with different numbers of positive charges and different hydrophobicity as standards. The

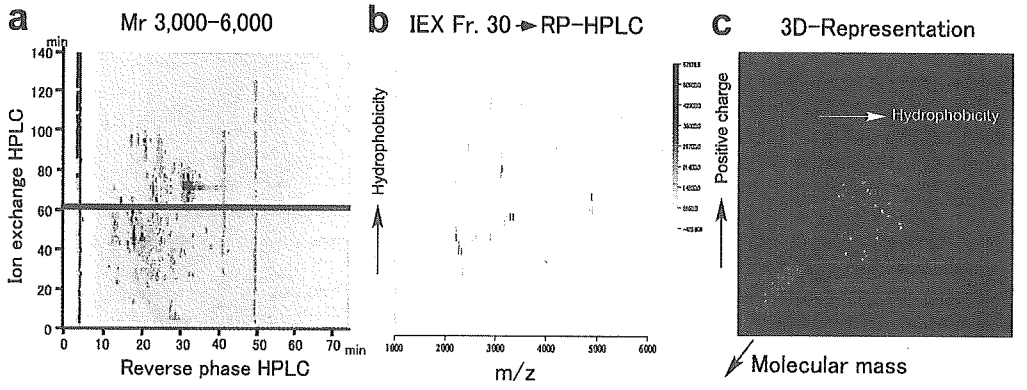

Figure 2. Analysis data for the pig brain peptides of 3,000<Mr<6,000. The peptides were separated by 2D-HPLC (a), analyzed by the mass spectrometers (b), and finally shown in the virtual 3D-space (c).

positive charge is estimated based on the elution times of the standard peptides, and the hydrophobicity is expressed as a percent CH_3CN concentration where the peptide is eluted.

In Fig. 2, the analysis data for the pig brain peptides of 3,000<Mr<6,000 are indicated step by step. Fig. 2a shows the 2D-HPLC profile of the peptides prepared from 5 g equivalents of the tissue. The absorbance at 210 nm is indicated by the density. Fraction 30 eluted at 60-62 min was then separated by reverse phase HPLC and each fraction was analyzed by the MALDI-TOF. MS analysis data of each fraction are serially plotted against m/z in Fig. 2b, and the density indicates the ion count. Bands with different density indicate the peptides. By accumulating 70 figures like the middle panel, all peptides are drawn in the virtual 3D-space composed of hydrophobicity, positive charge and molecular mass, as shown in Fig. 2c. By the aid of the software, we can freely rotate, zoom in and out this 3D drawing. If you click one ball, you will be able to check the peptide data and information so far as it has been sequenced and annotated.

In the case of pig brain peptides, we analyzed 2 g equivalents of the tissue, and detected 6,573 and 10,215 peptides in the Mr<3,000 and 3,000<Mr<6,000 fractions, respectively. As for about 25% of the detected peptides, the structural information is assumed to be obtained by the MS analysis, although a portion of them has been determined. In the case of mouse brain, we have so far analyzed the peptides in the Mr<3,000 fraction using 0.8 g equivalent of the tissue and detected 4,058 peptides. Among them, about 500 peptide sequences have been determined, and these data are available through the web page of the Peptidome project (www.peptidome.org).

In the case of mouse brain peptides, about 20% of the sequenced peptides are derived from the peptide hormone precursors and the secretory proteins. However, most of other peptides are derived from cytoplasmic, nuclear, mitochondorial, membrane proteins and so on. Several examples of the peptide/precursor relationship are shown in Fig. 3. The peptides derived from proenkephalin A, protachykinin and proopiomelanocortin are considered to be cleaved by prohormone convertases (PC), i.e. cleaved at the consecutive basic amino acids. In the cocaine- and amphetamine regulated transcript (CART), the peptide cleaved at the single arginine residues is observed, and many possible degradation products are detected in the case of procholecystokinin. We found that the regular secretory protein is processed in a

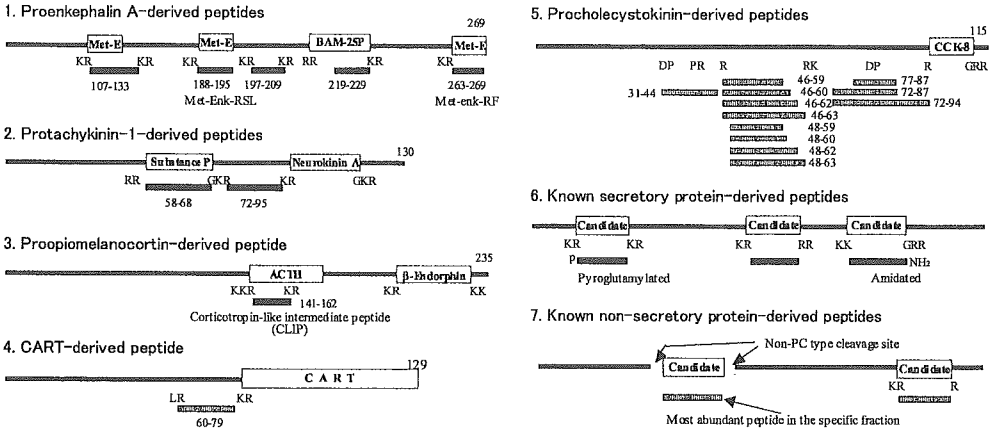

Figure 3. Examples of the peptides identified in the mouse brain extracts. Most peptides derived from the hormone precursor are cleaved by the PCs, but some unique processing patterns are also observed in other cases.

manner similar to that of the peptide hormone precursor. In another case, a unique peptide is present with high abundance but is not flanked by typical processing signals. Although it is necessary to confirm whether these peptides are endogenously present, I am sure that these data will help elucidate endogenous molecular forms and processing profiles of peptides and proteins.

To measure the biological activity, more amounts of peptides are required as compared with those used for the MS analysis even if the highly sensitive screening system is employed. We also separated the pig brain peptides by the large scale 2D-HPLC under the conditions identical to the peptide analysis. An aliquot of each fraction was submitted to the screening, and another aliquot was subjected to the MS analysis to confirm the elution positions. By utilizing the normalized 2D-HPLC as a common platform, data for endogenous peptides, biological activity and their related information can be accumulated, which is expected to increase the chance of discovery of the new bioactive peptides [2,3].

Recently, three groups reported that comprehensive analysis of peptides in the cell, tissue and body fluid can provide valuable information of the endogenous peptides [4-6]. Accumulation of these data in the common database will give us the solid basement for discovery of unidentified endogenous and bioactive peptides.

References

1. Minamino, N., Tanaka, J., Kuwahara, H., Kihara, T., Satomi, Y., Matsubae, M., and Takao, T. (2003) *J. Chromatogr. B*, **792**, 33-48.
2. Katafuchi, T., Kikumoto, K., Hamano, K., Kangawa, K., Matsuo, H., and Minamino, N. (2003) *J. Biol. Chem.*, **278**, 12046-12054.
3. Takeda, S., Okada, T., Okamura, M., Haga, T., Isoyama-Tanaka, J., Kuwahara, H., and Minamino, N. (2004) *J. Biochem.*, **135**, 597-604.
4. Schrader, M. and Schulz-Knappe, P. (2003) *Trends in Biotechnol.*, **19**, S55-S60.
5. Clynen, E., De Loof, A., and Schoofs, L. (2003) *Gen. Comp. Endocrinol.*, **132**, 1-9.
6. Svensson, M., Skold, K., Svenningsson, P., and Andren, P.E. (2003) *J. Proteome Res.*, **2**, 213-219.

循環器病学におけるペプチドミクス

佐々木一樹*, 南野直人*
SASAKI Kazuki, MINAMINO Naoto
*国立循環器病センター研究所薬理部

SUMMARY

生理活性ペプチドは循環器疾患の創薬，診断法のシーズとしての有用性が認識されている．ゲノム配列が明らかになった現在も未知の生理活性ペプチドの発見が期待されている．ペプチドミクスは生理活性ペプチドをはじめとした生体に内在するペプチドを包括的に理解するための新しい領域で，現状では発現解析法の確立に主眼が置かれている．新規生理活性ペプチドを発見するためには内在ペプチドの同定が必須であり，それはプロテオミクスでは現実的には不可能である．新規ペプチド発見の新しいアプローチとしてペプチドミクスが市民権を得る時代が到来しようとしている．

POINTS

●循環器疾患の診断・治療法開発のうえでペプチドは今後も有望である．
●ペプチドミクスは，生理活性ペプチド等の生体内に存在するペプチドを対象にする．
●プロテオミクスの手法ではこのようなペプチドは分析できない．
●ペプチドミクスは新規生理活性ペプチド探索の新しいアプローチを提供する．

KEY WORDS

ペプチドミクス，発現解析，生理活性ペプチド，疾患マーカー

はじめに

循環器系の調節因子として，アンジオテンシン，ナトリウム利尿ペプチド類，エンドセリン，アドレノメデュリン（AM）などを標的にした診断・治療法が開発されている．これらは分子量1万以下の小さな蛋白質，すなわちペプチドとよばれる．ペプチドミクスは，生理活性ペプチドをはじめとした生体に内在するペプチドの体系的な解析に関する技術の総称で，循環器病の領域では新規生理活性ペプチドの探索に貢献しうる．内在ペプチドの解析はプロテオミクスでは盲点になっており，本稿ではプロテオミクスとの差異について言及しながら，発現解析のツールとしてのペプチドミクスについて解説するとともに，低分子量蛋白質・ペプチド性の疾患マーカー探索の試みについても紹介する．

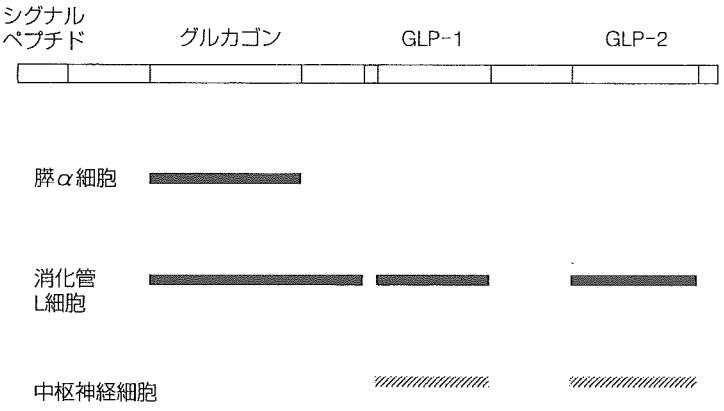

図❶　生理活性ペプチドのプロセシングの多様性
グルカゴンの事例．GLP：Glucagon-like peptide
（筆者作成）

本稿で用いる言葉の定義

ペプチドと蛋白質を区別する明解な定義はないが，一般にはゲル電気泳動で分離，検出されにくい分子量1万以下のアミノ酸のポリマーをペプチドと称する．ペプチドミクスは生体に内在するペプチドの体系的な解析に関する技術で，発現プロテオミクスが対象にしている蛋白質の酵素消化に由来するペプチドは除外される．また，ある系に存在する蛋白質全体をプロテオームと称し，それに対応してペプチド全体をペプチドームと称する．

生体内にどんなペプチドが存在するか

筆者ら[1)~3)]は1999年よりブタ脳を対象にペプチドーム解析を開始した．その結果から推定すると，体内に存在するペプチドの大部分は蛋白質の代謝過程で生じる分解ペプチドであると予想される．そのなかに，「積極的な存在意義」をもったペプチドが微量ながら存在している．医学の立場からは後者，すなわち，特定のアミノ酸配列を認識するプロテアーゼによる切断（プロセシング）に伴って生成するペプチドに興味がもたれる．たとえば，酵素前駆体が活性型に変換される際に随伴して切り出されるプロペプチドや，ペプチドホルモンなどとして知られる生理活性ペプチド，あるいは免疫系細胞のプロテアソームで分解されて主要組織適合性抗原と複合体を形成し抗原提示される10残基程度からなるペプチドなどである．

なかでも，ナトリウム利尿ペプチドやエンドセリンなどの生理活性ペプチドは循環器病の領域で注目される．生理活性ペプチドは，前駆体蛋白質から翻訳された後に，特定のアミノ酸配列を認識するプロテアーゼで切り出されて生じる．そして，特有の翻訳後修飾を伴うことが多く，ほとんどの事例で，その翻訳後修飾が生理活性の発現に必須である．たとえば，強力な摂食亢進作用以外に，重症心不全に対する心機能改善効果を有するグレリンはそのセリン残基がオクタン酸エステル化されており，血管拡張作用や心筋梗塞後の組織保護作用を示すAMは分子内環状構造とアミド化構造を有する．ゲノム情報のみではこのような翻訳後修飾や，組織ごとに異なるプロセシングパターン（図❶）は予測できず，構造解析も含めた発現解析の重要性を示している．したがって，ヒトでゲノム構造がほぼ明らかになったとはいえ，未知の生理活性ペプチドが今後も多数発見されると予想される．

ペプチドミクスとは

ペプチドミクスについて説明する前に，プロテオミクスについて簡単に言及する．これは蛋白質の個別研究ではなく，特定の系に存在する全蛋白質を対象にした発現解析や，構造と機能の相関を体系的に解析するための諸技術を示す言葉である．

一方で，ペプチドミクスは言葉自体が新しく，プロテ

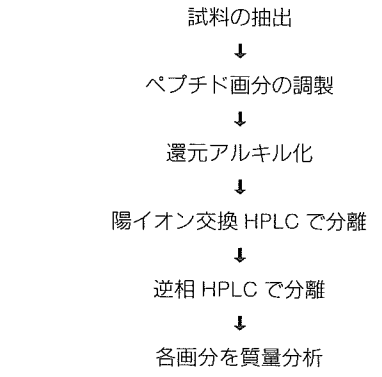

図❷ ペプチドミクスを用いる発現解析の流れ
(筆者作成)

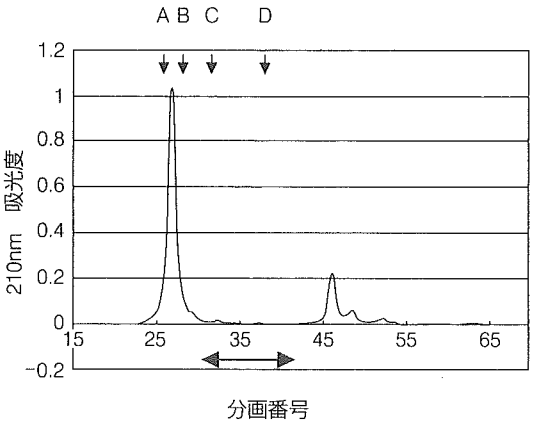

図❸ 培養細胞の上清を逆相系樹脂で処理した試料のゲル濾過
両矢印の領域がペプチド画分に相当する．左側のピークは蛋白質，右側は低分子物質．縦矢印は，分子量マーカーの位置：A, 血清アルブミン（約 66,000）；B, RNase A（約 13,500）；C, 神経ペプチド Y（4,271）；D, ニューロテンシン（1,673）
(筆者作成)

オミクスと同一視されやすい．現在は内在ペプチドの発現解析がペプチドミクスの最も大きな課題であり，生理活性ペプチドの新しい探索法として今後が期待されている．発現解析の流れを図❷に示す．試料ペプチドを高速液体クロマトグラフィ（high performance liquid chromatography：HPLC）で分離し，各分画の質量分析をおこない，含有されるペプチドの一次構造決定はタンデム質量分析とよばれる手法で進めていく．質量分析計および周辺技術の発展がペプチドミクスの中核をなしている．

ペプチドミクスとプロテオミクスの相違点

発現解析の領域に限定すると，プロテオミクスとペプチドミクスの端的な違いは，ペプチドミクスでは①分析試料から蛋白質成分を分離除去する，②分析試料は酵素消化を実施しない，の 2 点にある．

まず，①の背景について述べる．生物試料に含まれるペプチド総量は，蛋白質総量にくらべて非常に少ない．ブタ脳組織を対象とした筆者らの解析では，ペプチド画分の総重量は蛋白質画分の 0.1%程度であった．ほかの生物試料でも状況は同様である．図❸は，細胞の培養上清の事例で，ペプチドは蛋白質にくらべて少ないことが実感される．質量分析法で検出する場合，共存成分との相対的存在量比によって，当該分子の検出は大きく左右される．したがって発現解析に際してペプチド試料への蛋白質の混入はできうるかぎり排除する必要がある．蛋白質とペプチドの分離は，ゲル濾過，電気泳動ゲルからの electroelution，限外濾過などの方法がある．

つぎに②について説明する前に，プロテオミクスで酵素消化をおこなう理由を述べる．現在の質量分析計では，分子量の制約により，蛋白質自体をタンデム質量分析できないため，酵素消化が実施される．酵素消化にはトリプシンや LysC のように塩基性アミノ酸の C 末端側で切断する酵素が用いられるが，それによって構造解析（タンデム質量分析）時のデータ解釈が多少容易となる．ペプチドミクスはこのような酵素消化を加えることができない．生理活性ペプチドは塩基性アミノ酸を配列中に含むため，このような酵素で切断すると，ペプチド全体の構造を同定できなくなるからである（図❹）．

検出

前述のように，HPLC で分離された試料の質量分析がペプチドの発現解析の主要な作業を占めている．質量分析は高感度でペプチドを検出でき，ペプチドによっては 10 fmol という微量で検出可能である．しかし，これは実際の試料では実現しにくい状況である．たとえば，目的ペプチドを単一状態で 10 fmol 含む試料で良好な s/n で

[MKSIYFVAGLFVMLVQGSWQ] QDTEEKSRSLRSFSASQADPLSDPDQMNEDKRHSQGTFTSDYSKYLDSRR
AQDFVQWLMNTKRNRNNIAKRHDEFERHAEGTFTSDVSSYLEGQAAKEFIAWLVKGRGRRDFPEEVAIVEEL
GRRHADGSFSDEMNTILDNLAARDFINWLIQTKITDRK

図❹ 生理活性ペプチド前駆体のアミノ酸配列
グルカゴンの事例．太文字は生理活性ペプチドとして切り出される領域．括弧内はシグナルペプチド．プロテオミクスの手法では，酵素消化が必須のため，図中のRおよびKのC末端側で切断されてしまう．
（筆者作成）

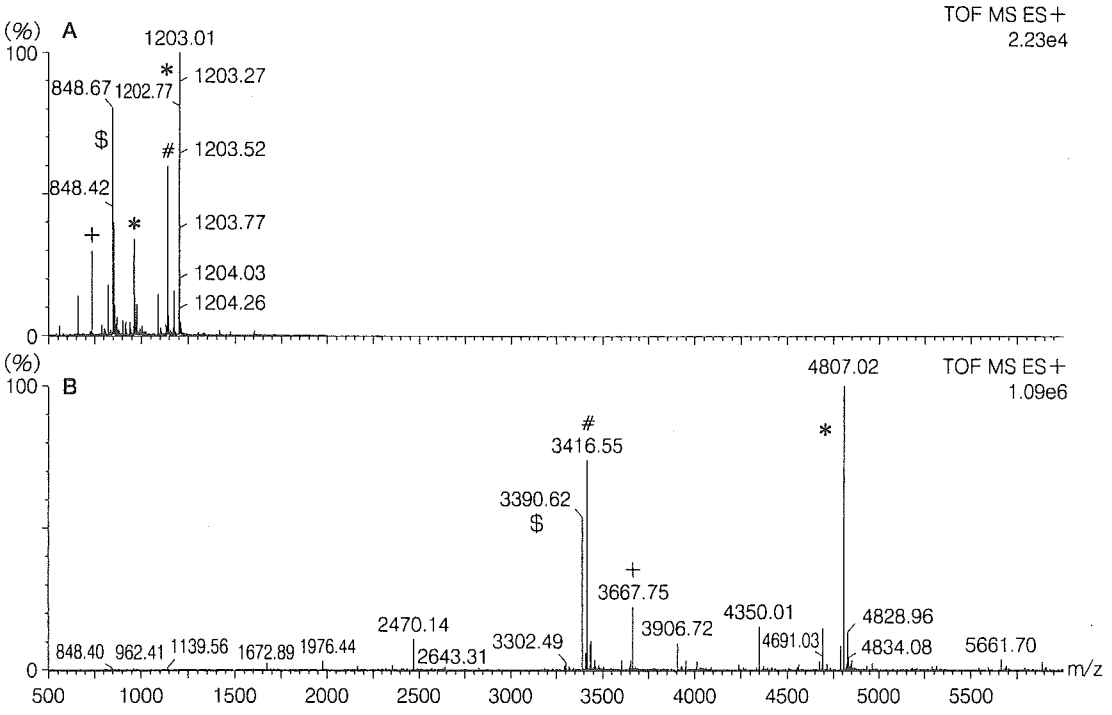

図❺ ESIによるマススペクトルの実際
A：測定で得られるスペクトル．B：Aで観測されるピークを1価に換算したスペクトル．たとえば，Bの＊印で示したペプチドは実際に検出されるわけではなく，実際にはAでみられるように4価，5価イオンのみが観測されている．同様に，Bで#印で示したペプチドは3価イオンのみが観測されている．
（筆者作成）

ピークが観測されたとしても，数十pmolで別のペプチドが共存すると，目的ペプチドの検出強度が顕著に低下する．この現象はイオン抑制とよばれる．イオン抑制効果を最小限にするためには，HPLCを用いてさまざまなパラメータでペプチドを分離する必要がある．

イオン化法は，マトリックス支援レーザー脱離イオン化（matrix assisted laser desorption/ionization：MALDI）と，エレクトロスプレーイオン化（electrospray ionization：ESI）の2種類を併用すると，検出ペプチド数を増加できる．質量分析ではマススペクトルのかたちでデータが得られ，横軸は質量電荷比（m/z），縦軸は相対強度を示す．一般にMALDIでは1価のイオンが強く観察されるために，スペクトル中にどんなペプチドが検出されているか理解しやすい．一方で，ESIでは多価イオンを生じるため，スペクトルは複雑になるのが難点である（図❺）．

同定

検出されたペプチドは逐次同定していく．質量分析計

を用いる一次構造決定法がいくつかあるなかで，タンデム質量分析法が最も実用的である．タンデム質量分析法とは，目的分子をさまざまな方法で断片化させ，生成するイオン（フラグメントイオン）を質量分析して，本来の分子の構造を明らかにする方法である．ヒトのようにゲノム構造がほぼ明らかになった生物種では，タンデム質量分析法による一次構造の決定は，Edman分解およびそれに引きつづくcDNAクローニングに依存していた従来とは比較にならないほど簡便になった．たとえば，図❻では，タンデムマススペクトル上に現れた5つのアミノ酸残基に由来するピークの質量の値，アミノ酸配列，目的ペプチドの質量の情報のみで一意的に同定されている．

タンデム質量分析による同定の実用面での最大の長所は，目的ピークが単一に精製されている必要がないことである．たとえば，図❼の試料中には38種類のペプチドが含まれているが，生化学的な分離操作を加えずに30種類が同定された．Edman分解で問題になるN末端のブロックなどの影響も受けない．ただし，タンデム質量分析法は一種の「破壊分析」であり，目的分子が断片化しない場合や，断片化で生じるフラグメントイオンの情報が不十分な場合は同定不可能である．

ペプチドミクスによる発現解析の実際

発現解析に際しては，試料調製の成否が解析結果の質を左右する．生物試料にはプロテアーゼが多量に含まれ，抽出の過程でペプチドは分解されやすい．また，抽出の過程で蛋白質が分解すると，本来存在していた内在性ペプチドと区別が不可能になる．そこで，これらを抑制するために，組織の場合は迅速な加熱処理，凍結不可避の場合は粉末化後の煮沸，液体試料の場合は迅速な酸処理や蛋白質との分離などで，プロテアーゼを失活，除去させる．また，ジスルフィド結合で環状化した内側のアミノ酸配列情報をタンデム質量分析で得るためには，システイン残基の還元アルキル化が必須である．また，生体試料に含まれる塩類や，化学反応に用いる試薬はペプチドよりイオン化しやすく，ペプチドの検出を妨げるので質量分析前に除去する．

このように調製した試料中には，種類，含有量ともに多種多様なペプチドが混合状態で存在している．これらを可能なかぎり数多く同定することが，発現解析の重要な課題となる．そのためには，原理の異なる液体クロマトグラフィを組みあわせて試料を分離する．1分画に，ある程度の高いs/nをもつペプチドが数種類のみ再現性よく分離されれば理想的であるが，ペプチドによって存在量はさまざまで，その開きは優に10の6乗を超えるため，存在量が多いペプチドは複数の分画に分散する．相対的に存在量が少ないペプチドを同定するためには，もう一段階のHPLC操作を加える．現実的には，ゲル濾過で得られたペプチド画分をまとめて還元アルキル化処理をおこなった試料を引きつづきイオン交換HPLCで分離する．イオン交換HPLCの各分画を逆相HPLCで約50～100分画に分離する．

このように，原理の異なる2つのクロマトグラフィで分離することを，二次元クロマトグラフィと称する．筆者らは，マウス脳のペプチドーム解析では，脳組織0.8 gより出発して，一次元目に陽イオン交換HPLC（70画分），二次元目に逆相HPLC(75画分)，すなわち全体を約5,000画分に分割している．このときに約8,000個のペプチドを検出し，構造決定に至ったのは約1,000個だった．このようにHPLC操作を1つ加えると，解析すべき試料数は飛躍的に増加するため，現実的には，スクリーニングの「網目」をどの程度の細かさ・粗さにするかを試料ごとに検討する必要がある．

候補ペプチドの選択

同定されたペプチドのなかから，生理活性ペプチドに特徴的な翻訳後修飾，同定ペプチドに隣接するアミノ酸配列(切断酵素の認識配列)，ジスルフィド結合，アミノ酸組成をもとに，候補ペプチドを選択する．翻訳後修飾を有する候補分子の場合は，修飾構造選択的な抗体を作製する．免疫染色で当該ペプチドの分布，産生細胞を把握し，さらにそのペプチドが組織中に実在することを，放射免疫測定法（radioimmunoassay：RIA），および組織抽出物からの免疫沈降物の質量分析で確認する．RIAは高感度で定量性にすぐれている．後者はそれらの点では劣っているが，「免疫活性」の実体を理解できる点です

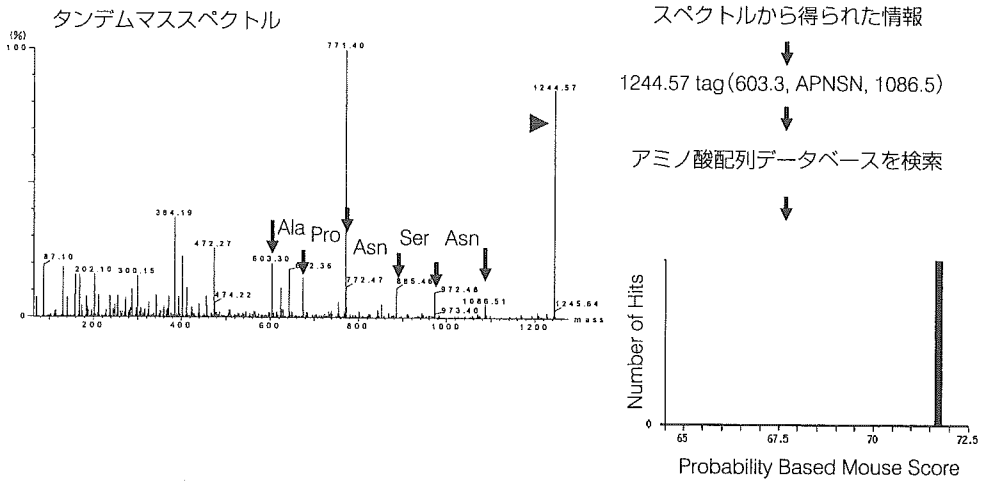

1. gi|4507243　Mass：12727　Total score：72　Peptides matched：1

somatostatin [Homo sapiens]

	Observed	Mr (expt)	Mr (calc)	Delta	Score	Peptide
1	1244.57	1243.56	1243.56	0.00	72	SA**NSNPA**MAPRE

図❻　m/z 1244.57（矢頭）のタンデム質量分析による同定
スペクトル上から連続した 5 つのアミノ酸配列を読み取り，質量の情報とともにデータベースを検索した．太文字の配列を含むペプチドとして一意的に同定された．
（筆者作成）

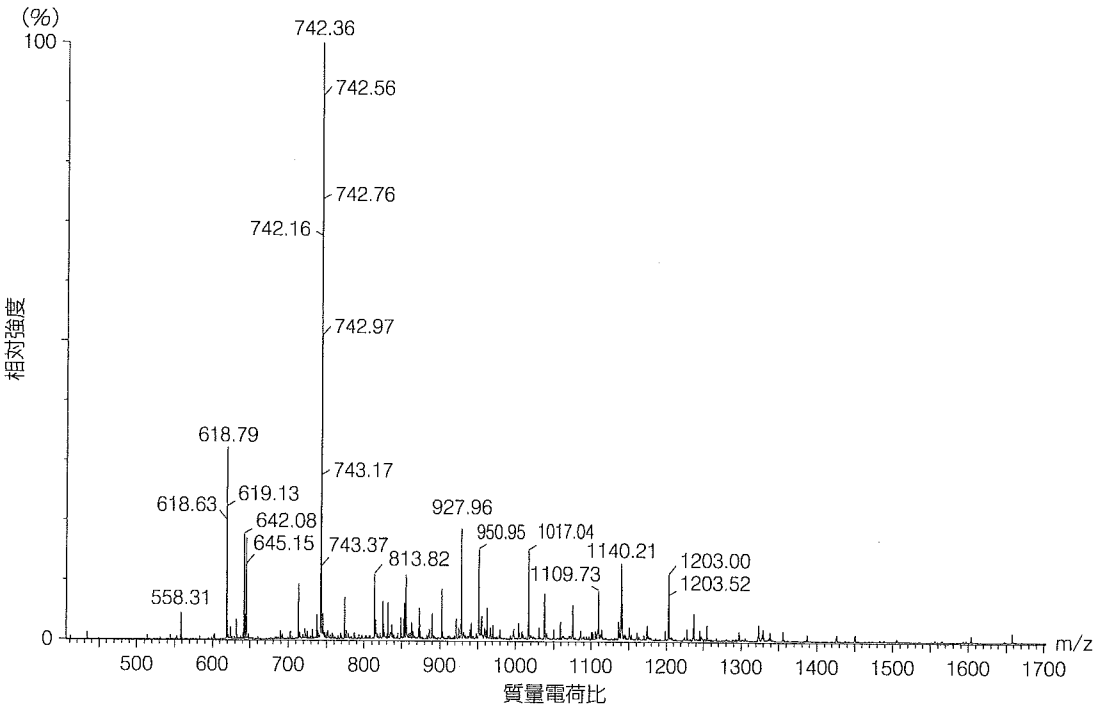

図❼　ペプチドミクスで実際に解析する試料の測定例
質量が測定できた 38 種類のペプチドのうち 30 個はこの試料からタンデム質量分析で同定された．
（筆者作成）

ぐれている[4].

実在を確認後に，どのような活性を有するかを検討する．特定の活性を指標に単離精製して発見されたペプチドとは異なり，この点は試行錯誤の要素が大きくなる．ただし，免疫染色で陽性となる細胞，組織の機能，あるいはその産物から，当該ペプチドの機能は推定も可能である．また，候補ペプチドについて，オーファン受容体のリガンドスクリーニングは受容体同定を考えるうえで望ましい．

上述の方法とは異なり，二次元に分離した各分画について，特定の生物活性で評価する方法も可能性があるが，多量に存在する既知の生理活性ペプチドが複数の分画に分散すると，未知の生理活性ペプチドの活性はマスクされる可能性が強く，工夫を必要とする．候補ペプチドが循環器系に作用するか否かは，生理学的実験が必須であり，動物実験を経て，有用なペプチド候補を選択していく．

疾患マーカーの開発

最後に，低分子量蛋白質関連でとりわけ癌研究で活発に実施されている疾患マーカー探索開発について簡単に言及する．循環器疾患においても，とくに心疾患に関しては診断および治療方針の決定などに有用なマーカーの開発が望まれている．心不全の病態把握のマーカーとして血漿中BNP濃度の測定が保険適用になっており，生命予後の予知因子としても確立している．このようなマーカーがさらに発見され，複数のマーカーの測定によって個別的な診断が可能になれば臨床的意義は大きい．究極的にはプアリスク群を選択可能なマーカーが発見されれば望ましい．心筋細胞から分泌あるいは逸脱してくる蛋白質やペプチドは循環血中で希釈されるため，数百μlの血液検体からこのようなマーカーのプロテオミクス，ペプチドミクスによる探索は現実的には困難である．

これに対して，癌の領域で提唱されたアプローチであるが，血中に多量に存在する蛋白質の数種類の特異的断片のセットが，診断に利用可能であるという成績が多数報告されている[5][6]．これは，癌では早期から凝固，線溶系に異常をきたす場合が多いので，血中に多量に存在する蛋白質にも二次的に影響を与えた結果，スペクトルに変化が現れるのではないかと推定されている．このようなセットを選択するためにはバイオインフォマティクスのソフトウエアの支援が必要になる．循環器疾患の病態に適用可能か否かは今後の課題になるが，その検討には，表面改良型レーザー脱離イオン化質量分析法[6](surface-enhanced laser desorption/ionization：SELDI)やアルブミンに非共有結合的に付着している低分子蛋白質を分析するアプローチが欧米では実施されている[7]．血清は凝固の過程で多数のプロテアーゼが活性化されており，多数のペプチド性ピークが観測されたとしても，真の病態を反映しているか，採血以後の体外で生じたアーティファクトなのかについて，試料の採取を含めた厳格な管理が必須となる[8]．

おわりに

本稿ではプロテオミクスと混同されやすいペプチドミクスについて，総論的な解説を中心にすえながら，運用面での注意点についても言及した．ペプチドミクスが循環器病領域で期待される役割として現在のところ中心になっているのは，新規生理活性ペプチドの探索と疾患マーカー開発である．本稿がその現状について理解するための一助になれば幸いである．

文　献

1) 南野直人：ペプチドーム―生体内ペプチドのファクトデータベース化―．蛋白質核酸酵素46 (suppl 11)：S 1510-S 1517，2001
2) Minamino N *et al*：Determination of endogenous peptides in the porcine brain：possible construction of peptidome, a fact database for endogenous peptides. *J Chromatogr B Analyt Technol Biomed Life Sci* 792：33-48, 2003
3) 佐々木一樹ほか：ペプチドーム解析の現状と展望．実験医学増刊23：133-140，2005
4) Sasaki K *et al*：Peptidomics-based approach reveals the

secretion of the 29-residue COOH-terminal fragment of the putative tumor suppressor protein DMBT1 from pancreatic adenocarcinoma cell lines. *Cancer Res* 62：4894-4898, 2002

5) Li J *et al*：Proteomics and bioinformatics approaches for identification of serum biomarkers to detect breast cancer. *Clin Chem* 48：1296-1304, 2002

6) 佐々木一樹：SELDI-TOF-MSによる腫瘍マーカー探索とがん診断の試み．化学フロンティア10，化学同人，京都，2003，pp. 181-190

7) Stanley BA *et al*：Heart disease, clinical proteomics and mass spectrometry. *Dis Markers* 20：167-178, 2004

8) Tammen H *et al*：Peptidomic analysis of human blood specimens：comparison between plasma specimens and serum by differential peptide display. *Proteomics* 5：3414-3422, 2005

SASAKI Kazuki

ささき・かずき
北海道生まれ．東京大学医学部医学科卒，国立がんセンター研究所を経て，2004年より国立循環器病センター研究所．
研究テーマ：質量分析法による新規生理活性ペプチドの探索．
趣味：音楽・庭園鑑賞．
E-mail：ksasaki@ri.ncvc.go.jp

Available online at www.sciencedirect.com
SCIENCE DIRECT®
ELSEVIER
Biochemical and Biophysical Research Communications 330 (2005) 75–80
BBRC
www.elsevier.com/locate/ybbrc

Calcitonin receptor-stimulating peptide-1 regulates ion transport and growth of renal epithelial cell line LLC-PK$_1$

Kazumasa Hamano, Takeshi Katafuchi, Katsuro Kikumoto, Naoto Minamino *

National Cardiovascular Center Research Institute, 5-7-1 Fujishirodai, Suita, Osaka 565-8565, Japan

Received 18 February 2005

Abstract

Calcitonin receptor-stimulating peptide-1 (CRSP-1) is a peptide recently identified from porcine brain by monitoring the cAMP production through an endogenous calcitonin (CT) receptor in the renal epithelial cell line LLC-PK$_1$. Here we investigated the effects of CRSP-1 on the ion transport and growth of LLC-PK$_1$ cells. CRSP-1 inhibited the growth of LLC-PK$_1$ cells with a higher potency than porcine CT. CRSP-1 enhanced the uptake of $^{22}Na^+$ into LLC-PK$_1$ cells more strongly than did CT and slightly reduced the $^{45}Ca^{2+}$ uptake. The enhancement of the $^{22}Na^+$ uptake was abolished by 5-(*N*-ethyl-*N*-isopropyl) amiloride, a strong Na^+/H^+ exchanger (NHE) inhibitor for NHE1, even at a concentration of 1×10^{-8} M, although other ion transporter inhibitors did not affect the $^{22}Na^+$ uptake. These results indicate that CRSP-1 enhances the $^{22}Na^+$ uptake by the specific activation of NHE1. Taken together, CRSP-1 is considered to be a new regulator for the urinary ion excretion and renal epithelial cell growth.

Keywords: Calcitonin receptor-stimulating peptide; Calcitonin; Calcitonin receptor; cAMP; LLC-PK$_1$ cell; Na^+/H^+ exchanger; 5-(*N*-Ethyl-*N*-isopropyl) amiloride; cAMP-dependent protein kinase

Calcitonin receptor-stimulating peptide-1 (CRSP-1) is a strong and specific agonist for the calcitonin (CT) receptor, its stimulatory activity for the cAMP production is 10-fold and more than 100-fold stronger than porcine CT in LLC-PK$_1$ cells and COS-7 cells expressing the CT receptor, respectively [1].

Measurement of CRSP-1 concentration in various porcine tissues by radioimmunoassay showed that the pituitary gland and thyroid gland contain the highest levels of CRSP-1 in the pig, although this peptide is widely distributed throughout the central nervous system. In the in vivo experiment, the bolus administration of CRSP-1 into rats significantly reduced the plasma Ca^{2+} level. We assumed that the CRSP-1 secreted from the pituitary gland and thyroid gland into the systemic circulation stimulated the CT receptor and regulated the physiological events in the kidney and the bone. Thus, we focused on the effect of CRSP-1 on the renal function in this study. LLC-PK$_1$ is one of the most characterized renal tubular epithelial cell lines [2–4]. This cell line abundantly expresses the CT receptor [5] and is often used for the analysis of the cell physiological function of CT in the renal epithelial cells. As CRSP-1 stimulates the cAMP production in LLC-PK$_1$ cells more potently than does CT, we examined the effect of CRSP-1 on LLC-PK$_1$ cells to elucidate the cell physiological function of CRSP-1 in the renal epithelial. In this study, therefore, we investigated the effects of CRSP-1 on ion uptake into LLC-PK$_1$ cells and their growth.

Materials and methods

Materials. Synthetic CRSP-1 and salmon CT were prepared and purchased as described previously [1]. ^{125}I-labeled deoxybromouridine (^{125}I-DU), ^{22}NaCl, and $^{45}CaCl_2$ were purchased from Amersham

* Corresponding author. Fax: +81 6 6835 5349.
E-mail address: minamino@ri.ncvc.go.jp (N. Minamino).

0006-291X/$ - see front matter © 2005 Elsevier Inc. All rights reserved.
doi:10.1016/j.bbrc.2005.02.131

Biosciences (Buckingham, UK). Benzthiazide, furosemide, 4-acetamido-4′-isothiocyanostilbene-2,2′-disulfonic acid (SITS), bumetanide, and 5-(*N*-ethyl-*N*-isopropyl) amiloride (EIPA) were purchased from Sigma (St. Louis, MO, USA).

Cell culture. LLC-PK_1 cells and opossum kidney (OK) cells were cultured with Dulbecco's modified Eagle's medium (DMEM) and minimum essential medium, respectively, supplemented with 10% fetal bovine serum (FBS), 100 μg/ml penicillin, and 100 U/ml streptomycin in a humidified atmosphere of 95% air–5% CO_2 at 37 °C.

Measurement of cAMP production in LLC-PK_1 cells. LLC-PK_1 cells were harvested, seeded at a density of 1×10^5 cell/well on 48-well plates, and cultured for 24 h. The cells were washed twice with DMEM/Hepes (20 mM, pH 7.4) containing 0.5 mM of 3-isobutyl-1-methyl xanthine (IBMX, Sigma) and 0.05% bovine serum albumin (DMEM/Hepes/IBMX solution), and were incubated in the same medium for 30 min at 37 °C. The incubation medium was then replaced with 150 μl medium, in which the sample of interest was dissolved, and further incubated at 37 °C for another 30 min. Aliquots (100 μl) of the incubation media were succinylated, evaporated, and then submitted to radioimmunoassay for cAMP, as reported previously [1].

Measurement of ^{125}I-DU uptake into LLC-PK_1 cells. The cells were harvested, seeded at a density of 2×10^4 cell/well on 24-well plates, and cultured for 48 h. The cells at 70% confluence were washed with 0.5 ml serum-free DMEM, replaced with DMEM containing 10% FBS and the peptide of interest, and incubated for 2 h at 37 °C. Then, ^{125}I-DU (4×10^5 cpm/50 μl in the DMEM) was added and further incubated for 5 h at 37 °C. Following the incubation, the cells were washed twice with ice-cold phosphate-buffered saline, incubated on ice for 30 min with 5% trichloroacetic acid, washed twice with 99.5% ethanol, and then solubilized in a buffer containing 0.1 M NaOH, 2% Na_2CO_3, and 1% SDS (500 μl/well). The radioactivity in each well was counted using a γ counter (ARC-1000, Aloka, Tokyo, Japan).

Measurement of intracellular cAMP accumulation in OK cells. OK cells were harvested, seeded at a density of 2×10^5 cell/well on 24-well plates, and cultured for 24 h. Porcine CT receptor cDNA ligated into pcDNA 3.1 expression vector (Promega, Madison, WI, USA) was transfected into the OK cells using Lipofectamine Plus (Invitrogen, San Diego, CA, USA) according to the manufacturer's protocol, and further incubated for 24 h. The cells were washed twice with DMEM/Hepes/IBMX solution and incubated in the same medium for 30 min at 37 °C. The incubation medium was then replaced with 250 μl medium, in which the sample of interest was dissolved, and further incubated at 37 °C for another 10 min. Following the incubation, the medium was replaced with 99.5% ethanol, and the cells were frozen at −80 °C for 24 h. The cells were lysed by repeated pipetting, and the debris of the lysate was removed by centrifuging at 12,000*g* for 5 min. The supernatant was evaporated, and the resulting pellet was dissolved in DMEM/Hepes/IBMX solution. Aliquots (100 μl) of the incubation media were succinylated, evaporated, and then submitted to radioimmunoassay for cAMP as reported previously [1].

Measurement of $^{45}Ca^{2+}$ uptake into LLC-PK_1 cells. LLC-PK_1 cells were harvested, seeded at a density of 2×10^6 cells on 6-well plates, and cultured for 2 days. The cells were washed twice with a calcium-free Hanks' solution, and replaced with the calcium-free Hanks' solution containing $^{45}Ca^{2+}$ (37 kBq/ml), in the absence or presence of CRSP-1 at a concentration of 1×10^{-6} M. Following incubation at 37 °C for 10 min, the cells were washed three times with ice-cold washing buffer (140 mM KCl, 5 mM $MgCl_2$, 20 mM Hepes (pH 7.4), 80 mM sucrose, and 1 mM EGTA), and the radioactivity incorporated into the cells was measured using a Topcount scintillation counter (Packard, Meriden, CT, USA).

Measurement of $^{22}Na^+$ uptake into OK cells and LLC-PK_1 cells. OK cells expressing recombinant CT receptor or LLC-PK_1 cells were harvested, seeded at a density of 2×10^6 cells/well on 6-well plates, and cultured for 2 days. The cells were washed twice with a Hanks'-choline chloride solution (137 mM choline chloride, 5.4 mM KCl, 4.2 mM $NaHCO_3$, 3 mM Na_2HPO_4, 0.4 mM KH_2PO_4, 1.3 mM $CaCl_2$, 0.5 mM $MgCl_2$, 0.8 mM $MgSO_4$, 10 mM glucose, and 5 mM Hepes, pH 7.4). Then, the Hanks'-choline chloride-$^{22}Na^+$ (37 kBq/ml) solution containing CRSP-1 (1×10^{-8} -1×10^{-6} M) alone, one of ion transporter inhibitors (1×10^{-6} M) alone, CRSP-1 (1×10^{-6} M) and one of ion transporter inhibitors (1×10^{-6} M), or CRSP-1 (1×10^{-6} M) and EIPA (1×10^{8} -1×10^{-6} M) was administered. Following incubation at 37 °C for 10 min, the cells were washed three times with ice-cold saline, and the $^{22}Na^+$ uptake into the cells was measured using a γ-counter (Cobra 5003, Packard).

Statistical analysis. Statistical analysis was performed using a one-way analysis of variance with repeated measurements, combined with a multiple comparison (Scheffe's *F* test). These analyses were carried out using StatView 5.01 (SAS Institute, Cary, NC, USA). The data are expressed as means ± SEM. *P* values less than 0.05 were considered significant.

Results

Fig. 1A shows the dose-dependent elevation of cAMP levels in the LLC-PK_1 cells stimulated with porcine CRSP-1, salmon CT, and porcine CT. CRSP-1, as well

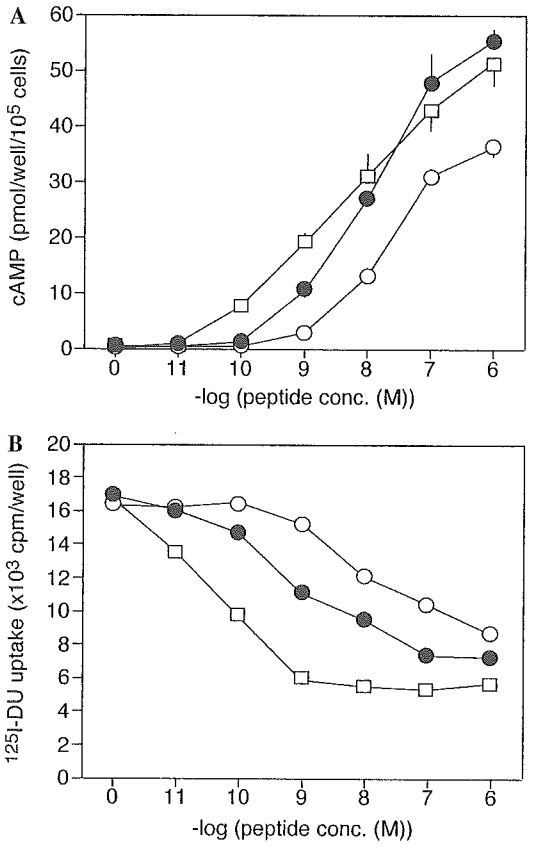

Fig. 1. Effects of CRSP-1, salmon CT, and porcine CT on cAMP production (A) and ^{125}I-DU uptake (B) into LLC-PK_1 cells. The cells were stimulated with porcine CRSP-1 (closed circle), salmon CT (open square) or porcine CT (open circle). (A) Dose-dependent increase of cAMP concentration in the culture medium of LLC-PK_1 cells. (B) Dose-dependent reduction of ^{125}I-DU uptake into LLC-PK_1 cells. Each point represents the mean ± SEM of three separate determinations.

as salmon CT and porcine CT, stimulated the cAMP production, and the potency order of the three peptides in the stimulatory activity of cAMP production was salmon CT > CRSP-1 > porcine CT. Since the increase of the intracellular cAMP concentration induces a change in growth of a variety of cell types, we next evaluated the effect of these peptides on the growth of the LLC-PK_1 cells by measuring the ^{125}I-DU uptake into chromosomal DNA. Parallel to the dose-dependent elevation of the cAMP production, these three peptides reduced the ^{125}I-DU uptake into LLC-PK_1 cells with the order of potency being salmon CT > CRSP-1 > porcine CT (Fig. 1B).

We next investigated the effects of CRSP-1 on ion transport. The effect of CRSP-1 on the $^{45}Ca^{2+}$ uptake into LLC-PK_1 cells is shown in Fig. 2. CRSP-1 significantly but weakly reduced the $^{45}Ca^{2+}$ uptake at a concentration of 1×10^{-6} M, and the effect of CRSP-1 on the reduction was weaker than that of salmon CT. A significant reduction of $^{45}Ca^{2+}$ uptake was not observed when LLC-PK_1 cells were stimulated with CRSP-1 at a concentration of 1×10^{-7} M (data not shown).

Fig. 3A shows the time course of $^{22}Na^{+}$ uptake into LLC-PK_1 cells in the absence or presence of CRSP-1. The $^{22}Na^{+}$ uptake into LLC-PK_1 cells was observed even at 0.1 min and reached a plateau at 60 min. When the cells were stimulated with CRSP-1 at a concentration of 1×10^{-7} M, the $^{22}Na^{+}$ uptake was significantly enhanced at 5 min and the enhancement reached a maximum at 10 min. Based on this result, we incubated the LLC-PK_1 cells with peptides and $^{22}Na^{+}$ for 10 min, and observed the enhancement of $^{22}Na^{+}$ uptake into the cells (Fig. 3B). CRSP-1 enhanced the $^{22}Na^{+}$ uptake into LLC-PK_1 cells from a concentration of 1×10^{-8} M. The potency order of the $^{22}Na^{+}$ uptake-increasing activity was salmon CT > CRSP-1 > porcine CT and was in agreement with that of cAMP production. Thus, we studied the effect of CRSP-1 on the $^{22}Na^{+}$ uptake in greater detail.

To verify that the activation of the CT receptor by CRSP-1 induces $^{22}Na^{+}$ uptake, porcine CT receptor

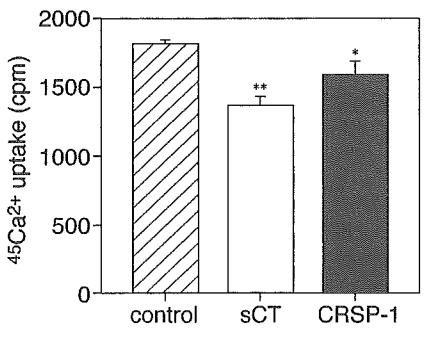

Fig. 2. Effects of CRSP-1, salmon CT, and porcine CT on $^{45}Ca^{2+}$ uptake. The cells were incubated with $^{45}Ca^{2+}$ only (control), with $^{45}Ca^{2+}$ and salmon CT (sCT, 1×10^{-6} M) or porcine CRSP-1 (CRSP-1, 1×10^{-6} M). Each bar represents the mean ± SEM of three separate determinations. $^{*}P < 0.05$; $^{**}P < 0.001$.

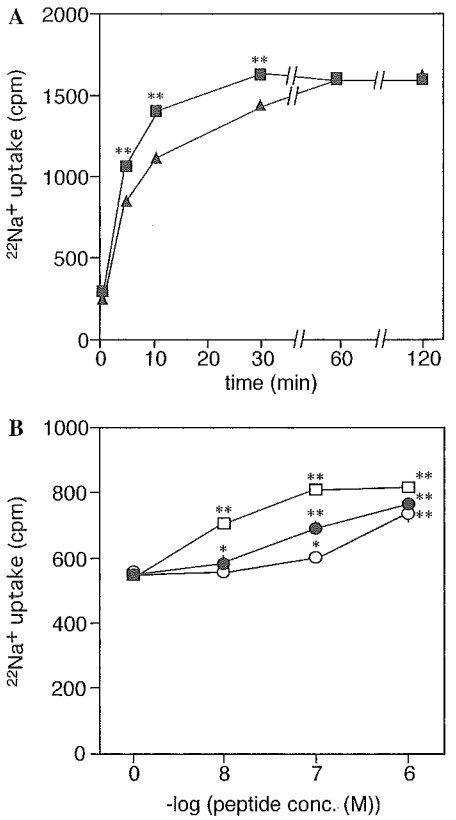

Fig. 3. Time course and dose-dependent enhancement of $^{22}Na^{+}$ uptake into LLC-PK_1 cells. (A) LLC-PK_1 cells were incubated with $^{22}Na^{+}$ in the absence (closed triangle) or presence of 1×10^{-7} M of CRSP-1 (closed square) for 0.1, 5, 10, 30, 60, and 120 min. (B) LLC-PK_1 cells were incubated with $^{22}Na^{+}$ only or with $^{22}Na^{+}$ and the indicated concentrations of porcine CRSP-1 (closed circle), salmon CT (open square), and porcine CT (open circle) for 10 min. Each point represents the mean ± SEM of three separate determinations. $^{*}P < 0.05$; $^{**}P < 0.001$.

cDNA inserted into mammalian expression vector (pcDNA-CTR) was transfected into OK cells, and the $^{22}Na^{+}$ uptake into the cells was measured in the presence of CRSP-1. CRSP-1 stimulated the cAMP production in OK cells, only when pcDNA-CTR was transfected into the cells (Fig. 4A). Parallel to the elevation of cAMP production, the $^{22}Na^{+}$ uptake into OK cells was enhanced with CRSP-1 (Fig. 4B). These results confirm that CRSP-1 actually enhanced the $^{22}Na^{+}$ uptake through the CT receptor-cAMP pathway.

To determine which Na^{+} transporter is activated with CRSP-1, we administered various transporter inhibitors, such as furosemide ($Na^{+}/K^{+}/Cl^{-}$ cotransporter inhibitor), benzthiazide (Na^{+}/Cl^{-} cotransporter inhibitor), EIPA (Na^{+}/H^{+} exchanger inhibitor), SITS (Cl^{-}/bicarbonate exchanger inhibitor), and bumetanide ($Na^{+}/K^{+}/Cl^{-}$ cotransporter inhibitor), into the culture medium of LLC-PK_1 cells at a concentration of 1×10^{-6} M, and measured their effects on the CRSP-1-induced $^{22}Na^{+}$ uptake. Although furosemide, bumetanide, benzthiazide or SITS did not alter the $^{22}Na^{+}$ uptake, EIPA abolished the